Supporting Information

EV-Lev: Extracellular Vesicle Isolation from Human Plasma Using Microfluidic Magnetic Levitation Device

Sena Yaman[a], Tessa Devoe[a,b], Ugur Aygun[c], Ugur Parlatan[c], Madhusudhan Reddy Bobbili[c,d,e], Asma H. Karim[c], Johannes Grillari[d,e] and Naside Gozde Durmus [a*]

[a.] *Molecular Imaging Program at Stanford (MIPS), Department of Radiology, Stanford University, Stanford, CA 94305-5281, USA.*
[b.] *Brown University, Providence, RI 02912, USA.*
[c.] *Canary Center for Cancer Early Detection, Department of Radiology, Stanford University, Stanford, CA 94304, USA.*
[d.] *Institute of Molecular Biotechnology, Department of Biotechnology, BOKU University, 1190 Wien, Austria.*
[e.] *Ludwig Boltzmann Institute for Traumatology, The Research Center in Cooperation with AUVA, 1200 Wien, Austria.*
**Corresponding author: Naside Gozde Durmus, PhD, gdurmus@stanford.edu*

Table S1. Cost estimation for EV-Lev platform

Component	Price	EV-Lev	Estimated Total
	Price (e.a.)		
Magnet	$5.75	$11.50	
Price (50-piece)			
Mirror	$33	$1.32	
	Price (e.a.)		
Needle	$0.40	$0.80	
	per sq ft		
PMMA	~$6	~$0.5	
	100 ft		
Tubing	~$100	$1	
			$14.62

Table S2. Theoretical maximum EV recovery using PS and PMMA beads using the average EV size of 100 nm which closely aligns with the measured sizes of eluted EVs

	Diameter (m)	**Surface Area (m^2)**	**EV cross sectional area (m^2)**	**Number of beads in the 1x bead solution**	**Total number of EVs that can be collected**	**Maximum EV concentration (in 100 µL elution buffer)**
Polystyrene (**PS**)	1×10^{-4}	3.14×10^{-8}	7.85×10^{-15}	218	8.72×10^{8}	8.72×10^{9} particle/mL
Poly(methyl methacrylate) (**PMMA**)	4×10^{-5}	5.03×10^{-9}	7.85×10^{-15}	1517	9.71×10^{8}	9.71×10^{9} particle/mL

Table S3. Comparison of size number for EVs eluted from different antibody and bead combinations using a t-test

Column B	PMMA-CD9
vs.	vs.
Column A	PS-CD9
Unpaired t test	
P value	0.7454
P value summary	ns
Significantly different (P < 0.05)?	No
One- or two-tailed P value?	Two-tailed
t, df	t=0.3479, df=4
How big is the difference?	
Mean of column A	106.8
Mean of column B	108.3
Difference between means (B - A) ± SEM	1.533 ± 4.407
95% confidence interval	-10.70 to 13.77
R squared (eta squared)	0.02937
F test to compare variances	
F, DFn, Dfd	44.88, 2, 2
P value	0.0436
P value summary	*
Significantly different (P < 0.05)?	Yes
Data analyzed	
Sample size, column A	3
Sample size, column B	3

Column B	PMMA-CD63
vs.	vs.
Column A	PS-CD63
Unpaired t test	
P value	0.1411
P value summary	ns
Significantly different (P < 0.05)?	No
One- or two-tailed P value?	Two-tailed
t, df	t=1.831, df=4
How big is the difference?	
Mean of column A	107.7
Mean of column B	103.9
Difference between means (B - A) ± SEM	-3.833 ± 2.094
95% confidence interval	-9.647 to 1.980
R squared (eta squared)	0.4559
F test to compare variances	
F, DFn, Dfd	2.769, 2, 2
P value	0.5307
P value summary	ns
Significantly different (P < 0.05)?	No
Data analyzed	
Sample size, column A	3
Sample size, column B	3

Column B	PMMA-CD81
vs.	vs.
Column A	PS-CD81
Unpaired t test	
P value	0.7603
P value summary	ns
Significantly different (P < 0.05)?	No
One- or two-tailed P value?	Two-tailed
t, df	t=0.3267, df=4
How big is the difference?	
Mean of column A	105.9
Mean of column B	103.6
Difference between means (B - A) ± SEM	-2.300 ± 7.041
95% confidence interval	-21.85 to 17.25
R squared (eta squared)	0.02599
F test to compare variances	
F, DFn, Dfd	1.474, 2, 2
P value	0.8083
P value summary	ns
Significantly different (P < 0.05)?	No
Data analyzed	
Sample size, column A	3
Sample size, column B	3

Table S4. Comparison of particle number for EVs eluted from different antibody and bead combinations using a t-test

Column B	PMMA-CD9
vs.	vs.
Column A	PS-CD9
Unpaired t test	
P value	0.5788
P value summary	ns
Significantly different (P < 0.05)?	No
One- or two-tailed P value?	Two-tailed
t, df	t=0.6033, df=4
How big is the difference?	
Mean of column A	21241481
Mean of column B	22130864
Difference between means (B - A) ± SEM	889383 ± 1474172
95% confidence interval	-3203575 to 4982341
R squared (eta squared)	0.08341
F test to compare variances	
F, DFn, Dfd	1.603, 2, 2
P value	0.7684
P value summary	ns
Significantly different (P < 0.05)?	No
Data analyzed	
Sample size, column A	3
Sample size, column B	3

Column B	PMMA-CD63
vs.	vs.
Column A	PS-CD63
Unpaired t test	
P value	0.7672
P value summary	ns
Significantly different (P < 0.05)?	No
One- or two-tailed P value?	Two-tailed
t, df	t=0.3169, df=4
How big is the difference?	
Mean of column A	23105556
Mean of column B	24444444
Difference between means (B - A) ± SEM	1338889 ± 4225426
95% confidence interval	-10392776 to 13070553
R squared (eta squared)	0.02449
F test to compare variances	
F, DFn, Dfd	2.950, 2, 2
P value	0.5064
P value summary	ns
Significantly different (P < 0.05)?	No
Data analyzed	
Sample size, column A	3
Sample size, column B	3

Column B	PMMA-CD81
vs.	vs.
Column A	PS-CD81
Unpaired t test	
P value	0.6492
P value summary	ns
Significantly different (P < 0.05)?	No
One- or two-tailed P value?	Two-tailed
t, df	t=0.4910, df=4
How big is the difference?	
Mean of column A	21503915
Mean of column B	19759259
Difference between means (B - A) ± SEM	-1744656 ± 3553339
95% confidence interval	-11610305 to 8120993
R squared (eta squared)	0.05684
F test to compare variances	
F, DFn, Dfd	4.559, 2, 2
P value	0.3598
P value summary	ns
Significantly different (P < 0.05)?	No
Data analyzed	
Sample size, column A	3
Sample size, column B	3

Table S5. Comparison of particle number of EVs eluted from the beads collected from top and bottom channels of EV-Lev and EVs collected by ultracentrifuge using an ordinary one-way ANOVA.

Number of families	1							
Number of comparisons per family	3							
Alpha	0.05							
Tukey's multiple comparisons test	Mean Diff.	95.00% CI of diff.	Below threshold?	Summary	Adjusted P Value			
Top vs. Bottom	-13056	-478703458 to 478677347	No	ns	>0.9999	A-B		
Top vs. UC	-1138915370	-1617605772 to -660224968	Yes	***	0.0002	A-C		
Bottom vs. UC	-1138902315	-1617592717 to -660211913	Yes	***	0.0002	B-C		
Test details	Mean 1	Mean 2	Mean Diff.	SE of diff.	n1	n2	q	DF
Top vs. Bottom	9834630	9847685	-13056	171450372	4	4	0.0001077	9
Top vs. UC	9834630	1148750000	-1138915370	171450372	4	4	9.394	9
Bottom vs. UC	9847685	1148750000	-1138902315	171450372	4	4	9.394	9
Compact letter display								
UC	A							
Bottom	B							
Top	B							

Table S6. Comparison of mean size for EVs eluted from the beads collected from top and bottom channels of EV-Lev and EVs collected by ultracentrifuge using an ordinary one-way ANOVA.

Number of families	1							
Number of comparisons per family	3							
Alpha	0.05							
Holm-Šídák's multiple comparisons te	Mean Diff.	Below threshold?	Summary	Adjusted P Value				
Top vs. Bottom	0	No	ns	>0.9999	A-B			
Top vs. UC	4.125	No	ns	0.7914	A-C			
Bottom vs. UC	4.125	No	ns	0.7914	B-C			
Test details	Mean 1	Mean 2	Mean Diff.	SE of diff.	n1	n2	t	DF
Top vs. Bottom	105.3	105.3	0	4.742	4	4	0	9
Top vs. UC	105.3	101.2	4.125	4.742	4	4	0.8699	9
Bottom vs. UC	105.3	101.2	4.125	4.742	4	4	0.8699	9
Compact letter display								
Top	A							
Bottom	A							
UC	A							

Principle of Co-Isolation of Extracellular Vesicles Using Polymeric Beads and Magnetic Levitation:

Magnetic levitation has proven to be a versatile tool for a variety of life science and biomedical applications[1-3]. It includes the utilization of micro and/or nano particles for biomolecule [4, 5], cell [5], and virus detection[6,7] within a confined space between two opposing magnets. The levitation of these particles is determined by the interplay of two forces, the buoyancy force and magnetic force, which depend on the particle's density and magnetic susceptibility. The strength of the magnetic force is proportional to the difference between the magnetic susceptibility of the particle and its surrounding paramagnetic medium. [4, 8] Polymer beads are inherently non-magnetic and tend to move away from higher magnetic field regions to lower (diamagnetic repulsion). Even though this effect is weak, it can be enhanced by submerging the particles in a paramagnetic agent, such as Gadolinium (Gd)[9]. Given the negligible the magnetic susceptibility of polymer beads compared to a paramagnetic medium with Gd, their levitation is solely based on their density: higher density polymer beads levitate closer to the bottom compared to their less dense counterparts[4,9,10] regardless of their size[4]. We leveraged this phenomenon to sort beads of different densities, each decorated with distinct surface markers to enable the co-isolation of different populations of extracellular vesicles.

"Theoretical Calculation of Maximum EV Binding for PS and PMMA beads:

To eliminate the heterogeneity in EV size, we employed an approach using the average EV size of 100 nm (which closely aligns with the measured sizes of eluted EVs). Our analysis in Table S2 assumes a uniform and complete coverage of the bead surface with EVs. According to the theoretical maximum calculations, PS and PMMA beads could capture 8.72x 10^8 and 9.71x 10^8 particle, respectively.

In the validation experiments with pre-purified EVs, the initial particle concentration was 8.50 × 10^{10} particles/mL. Concurrently, the maximum theoretical EV concentration (from **Table S2**) was calculated as 9.71 × 10^9 particles/mL for 40 μm PMMA. The experimental particle concentrations after elution from the beads were:

PMMA-CD9: 6.27 × 10^8 ± 1.01 × 10^8 particles/mL

PMMA-CD63: 7.04 × 10^8 ± 1.93 × 10^8 particles/mL

PMMA-CD81: 5.24 × 10^8 ± 2.88 × 10^8 particles/mL

We demonstrated the proof-of-principle for vesicle isolation using inexpensive polymer beads in a high-throughput, flow-based platform. The experimental results reveal a recovery yield ~1.3 order of magnitude lower than the theoretical maximum EV concentration. This discrepancy can be attributed to the initial assumption of complete bead surface coverage with EVs, which differs from the practical challenges of achieving whole surface functionalization with antibodies at the correct orientation. The EV-Lev system can process thousands of beads simultaneously, enabling the potential isolation of billions of vesicles, as validated in our experiments. To further increase the rate of recovery from the initial solution, total surface area that captures EVs might be increased by increasing the total number of antibody-coated beads in the solution.

For instance, increasing the number of 40 μm PMMA beads ten-fold to 15170, would theoretically allow capture of 9.71 × 10^9 EVs total.

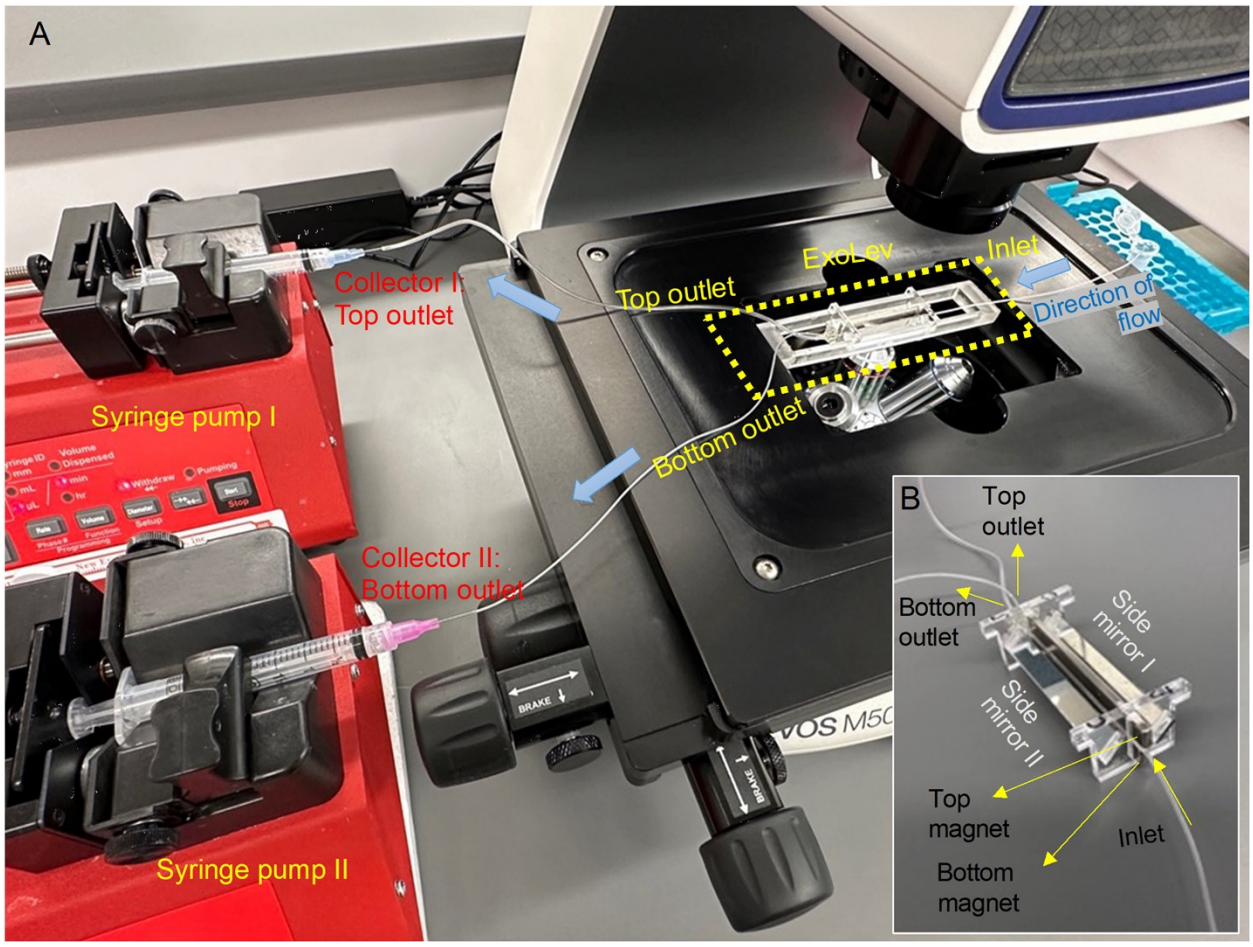

Figure S1: Photo of the EV-Lev-based sorting system**. A.** Top and bottom outlets are attached to two syringe pumps that operate at different flow rates. The EV-Lev platform is placed on a 3D printed holder that is mounted on an inverted microscope (EVOS M5000) and imaged during the sorting via two side-mirrors attached. **B.** Close-up photograph of EV-Lev sorter.

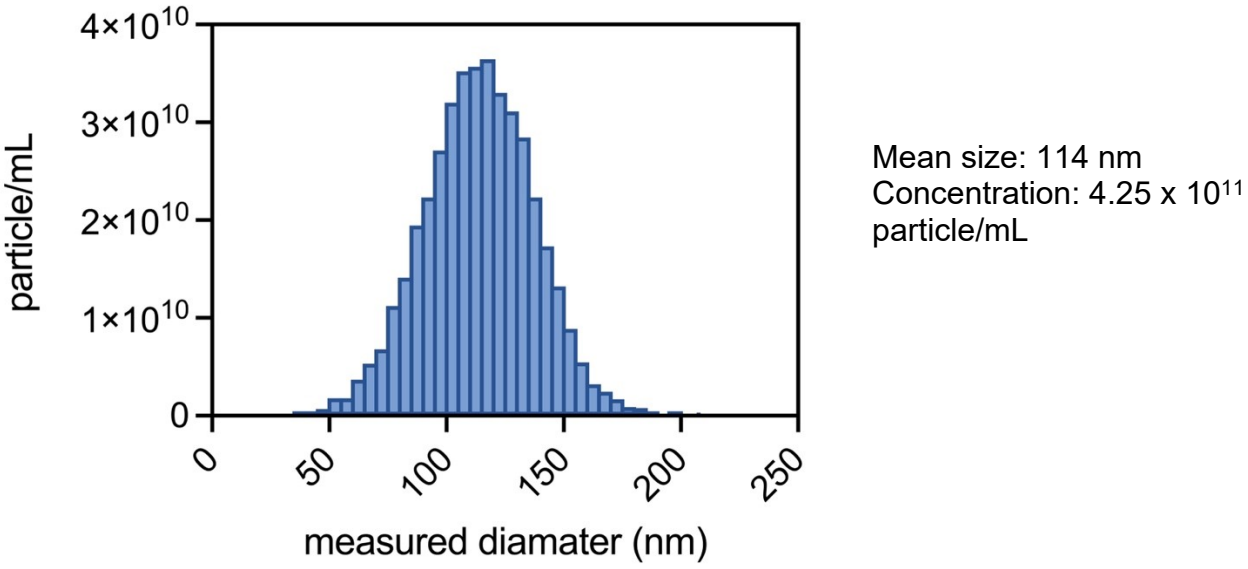

Figure S2. iSCAT analysis of particles collected after ExoTIC purification using 300 µL of plasma.

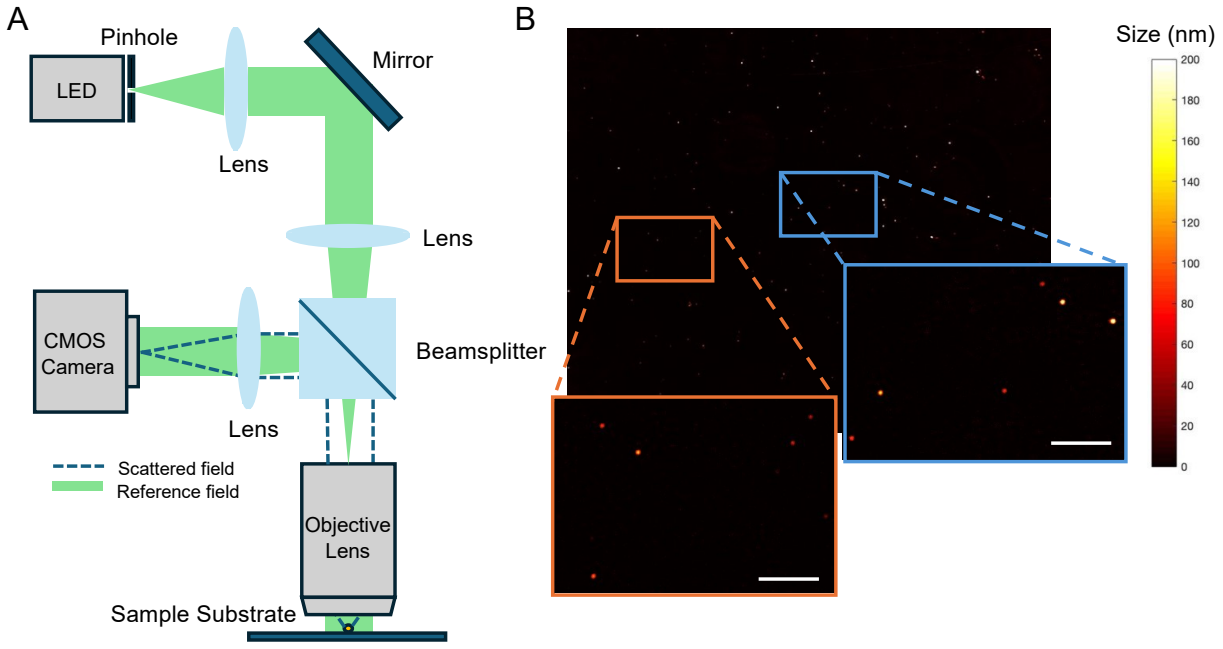

Figure S3: Interferometric scattering (iSCAT) microscopy measurements for EVs collected by EV-Lev. **A**. Schematic representation of configuration of the interferometric imaging system. **B.** Images of extracellular vesicles after elution from the beads. Scale bars: 5 µm

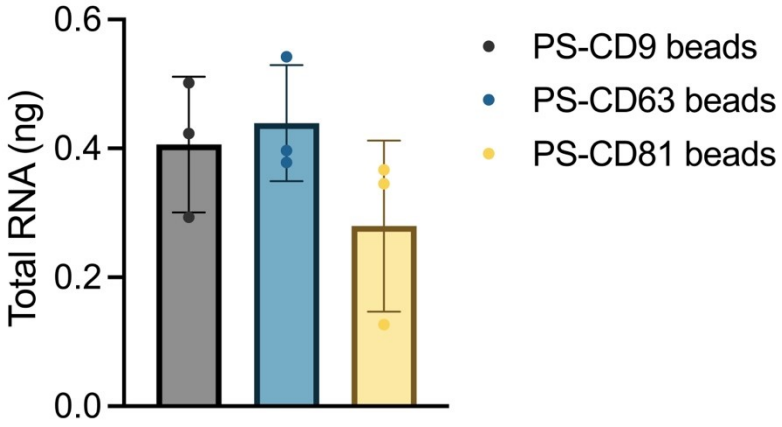

Figure S4: Total RNA content of eluting extracellular vesicles after the elution from Anti-CD9, -CD63, or CD81 beads using 20 µL of human plasma with 1 x of PS bead solution.

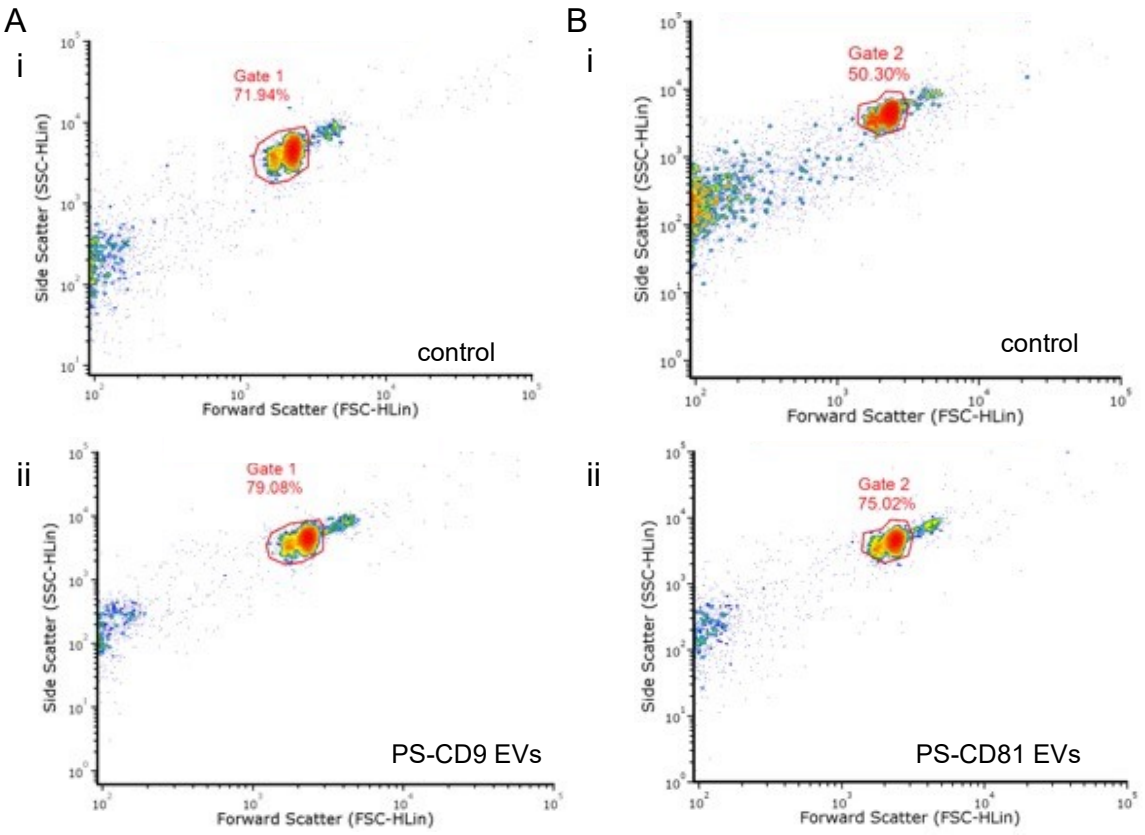

iii

Parameter	# of Events	% of all cells	% of gated cells (from plot)	Median
Red-R Fluorescence (RED-R-HLin)	3597	71.94	100.00	74.76
Red-R Fluorescence (RED-R-HLin)	3954	79.08	100.00	176.28

Parameter	# of Events	% of all cells	% of gated cells (from plot)	Median
Yellow-B Fluorescence (YEL-B-HLin)	3597	71.94	100.00	64.10
Yellow-B Fluorescence (YEL-B-HLin)	3954	79.08	100.00	729.02

iii

Parameter	# of Events	% of all cells	% of gated cells (from plot)	Median
Yellow-B Fluorescence (YEL-B-HLin)	2515	50.30	100.00	64.78
Yellow-B Fluorescence (YEL-B-HLin)	3751	75.02	100.00	107.79

Parameter	# of Events	% of all cells	% of gated cells (from plot)	Median
Red-R Fluorescence (RED-R-HLin)	2515	50.30	100.00	81.40
Red-R Fluorescence (RED-R-HLin)	3751	75.02	100.00	120.28

Figure S5: FC analysis of eluted from **A.** PS-CD9 or **B.** PS-CD81 beads. **i**, **ii**, and **iii** represent control, sample, and histogram statistics for each condition. Gate 1 and Gate 2 was set according to CD9 and CD81 magnetic bead populations in A-i and B-i, respectively. Red-Red or Yellow-Blue lasers were used for APC-CD9 or PE-CD81 stains, respectively.

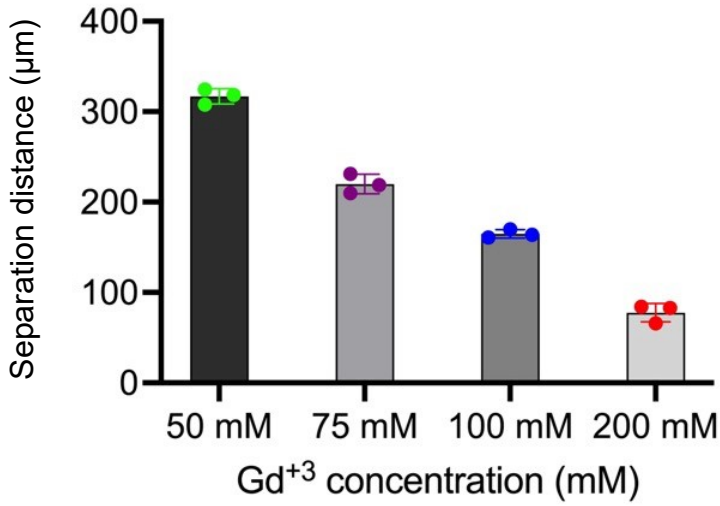

Figure S6: Separation distance of two different beads under different Gd concentrations

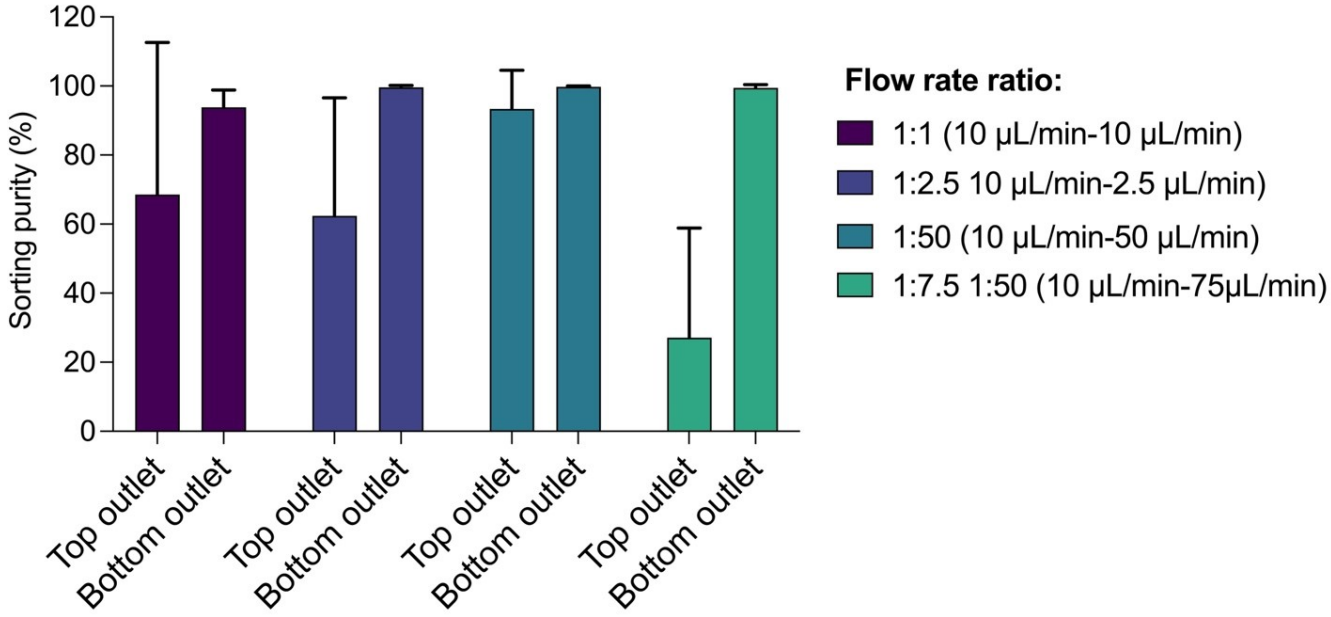

Figure S7: Optimization of flow rate in terms of top and bottom outlet purity for EV-Lev-based bead sorting at different flow rate ratios of bottom and top outlets using a mixture of streptavidin-coated PS and PMMA beads. Sorted polymer beads at top (PS) and bottom (PMMA) outlets placed in wells and counted to assess sorting purity.

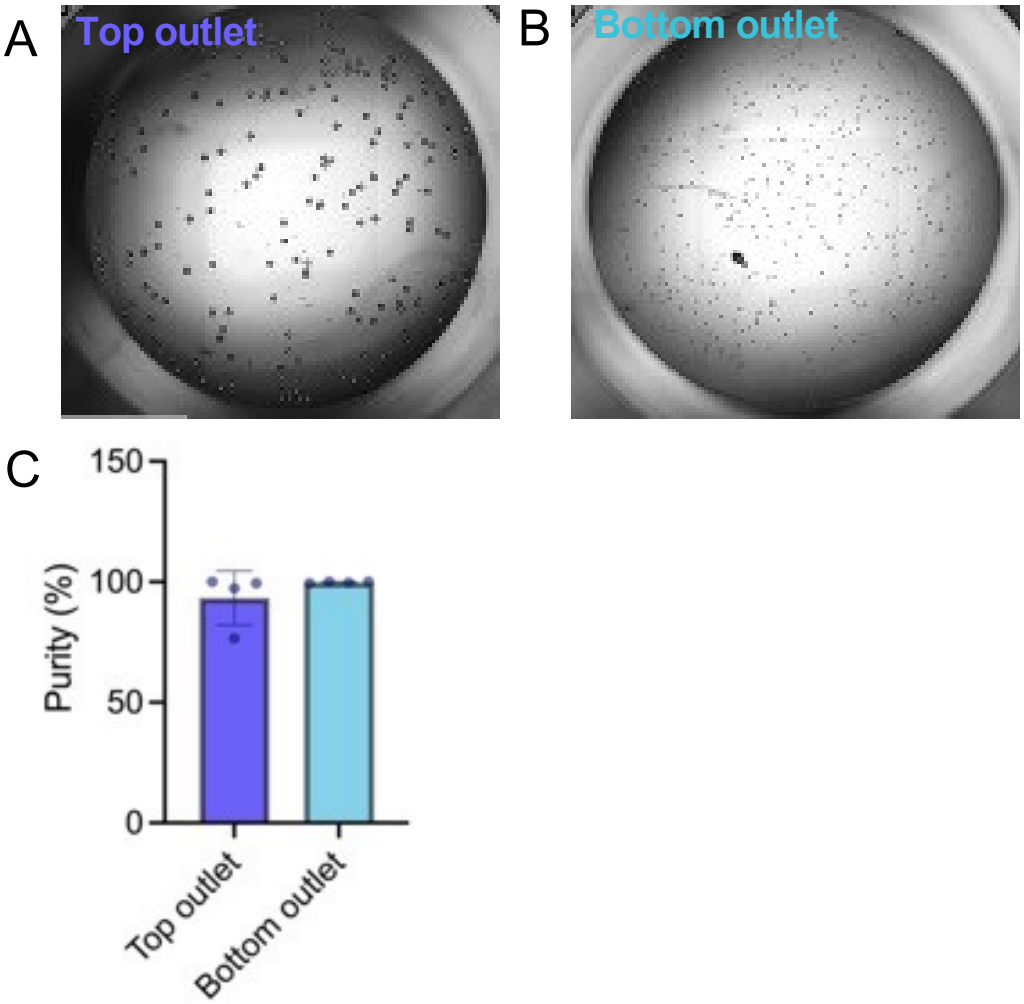

Figure S8: Sorted polymer beads at top and bottom outlets placed in wells and counted for purity for optimized flow rate: 50 µL/min for top and 10 µL/min for bottom channels, respectively. Photograph of the beads collected from **A.** top outlet and **B.** bottom outlet. **C.** Assessment of purity after the quantification of the beads from each outlet.

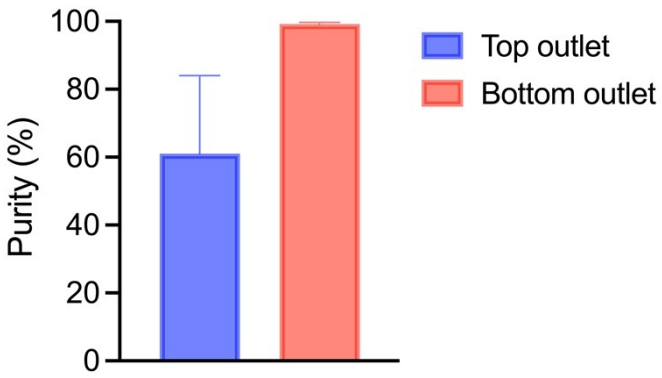

Figure S9: Sorting purity in top and bottom outlets after incubating human plasma sample with an anti-CD9 coated PS bead and anti-CD81 coated PMMA bead mixture.

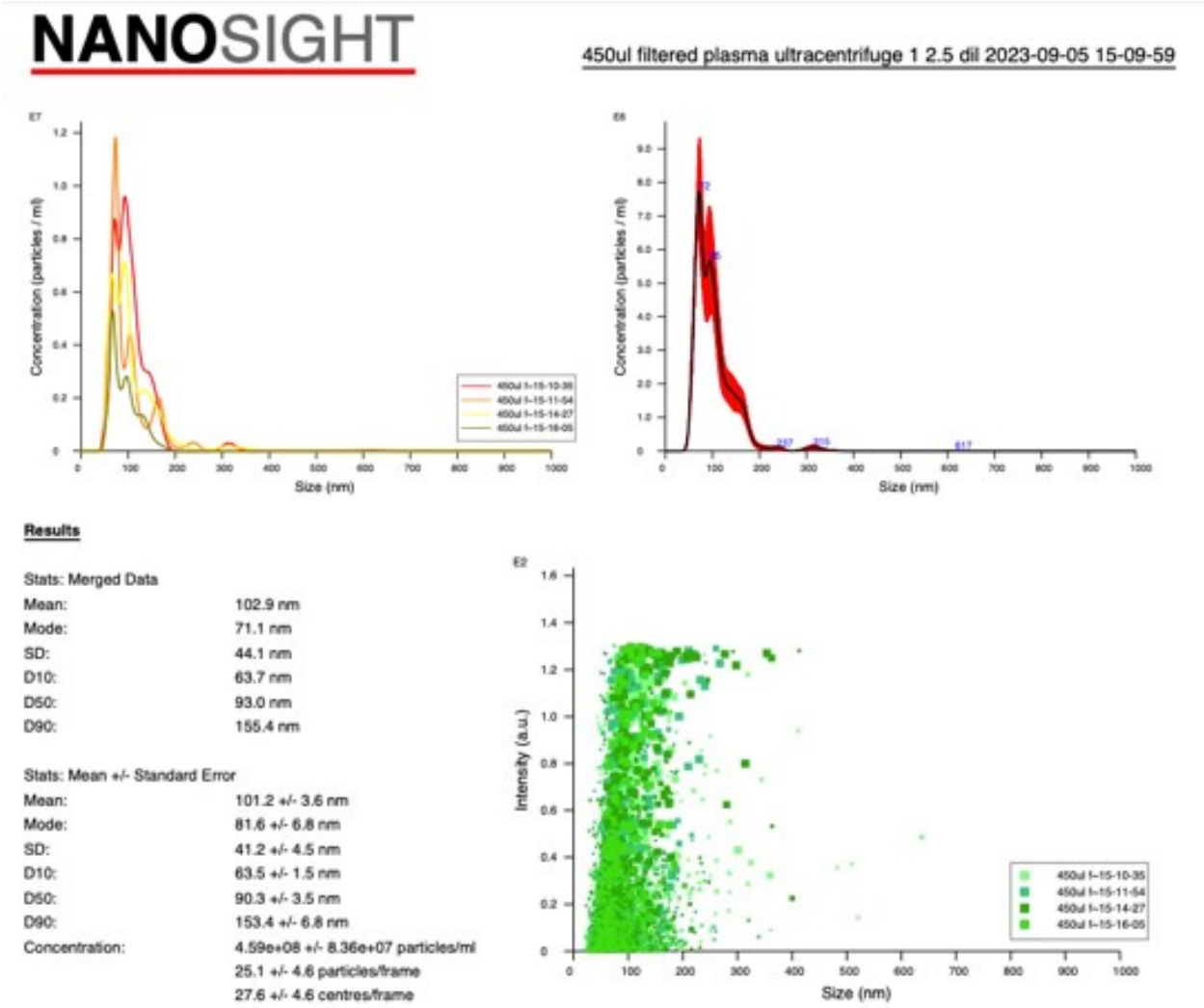

Figure S10: NTA measurement of EVs collected by ultracentrifuge using 450 µL of plasma diluted in a 1:2.5 ratio.

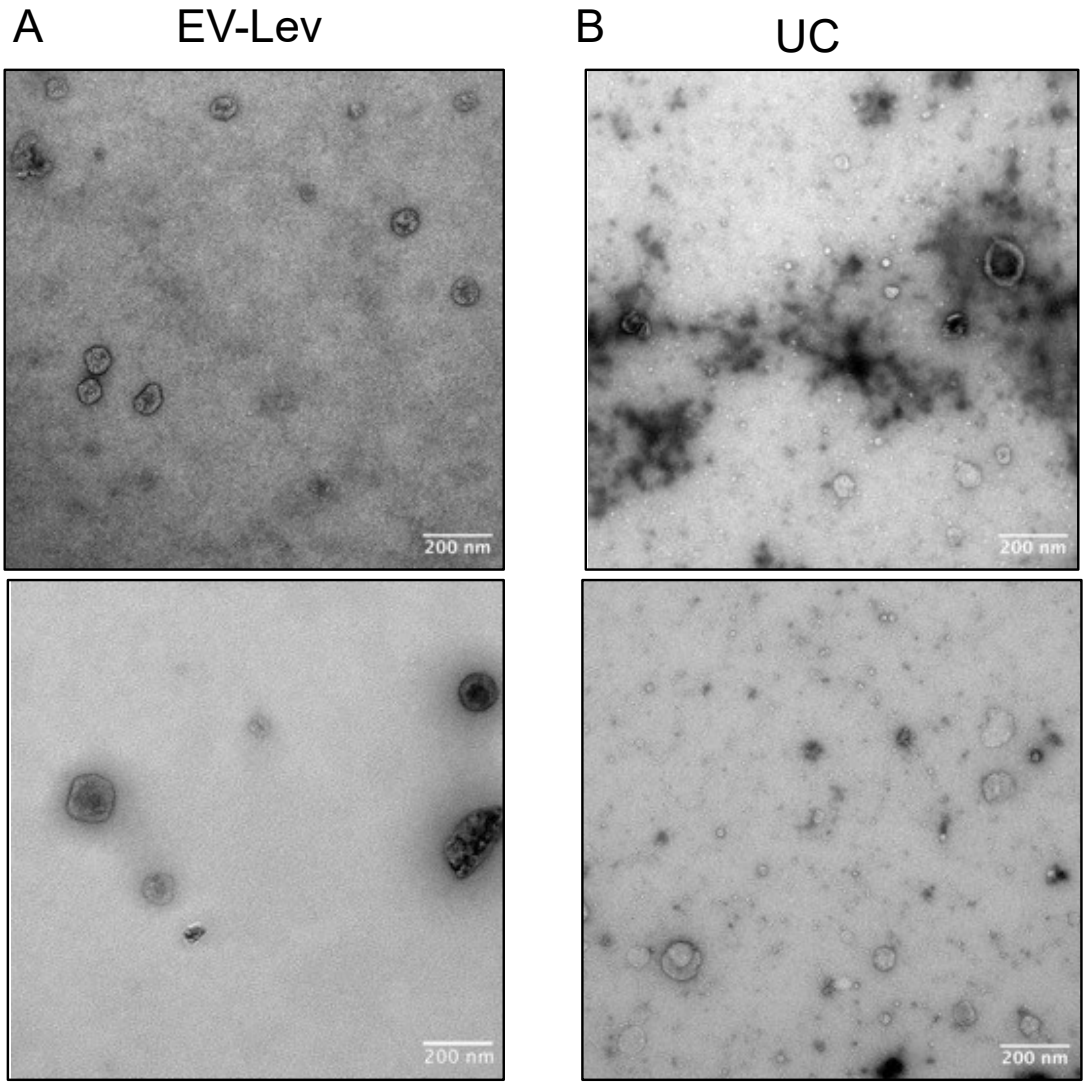

Figure S11: TEM images of extracellular vesicles collected by **A.** EV-Lev or **B.** Ultracentrifugation (UC). TEM images showing the much clean and uniform EVs isolated from human plasma using EV-Lev. In contrast, ultracentrifugation prepares EV in a mixture with small aggregates and debris. (Scale bars: 200 nm).

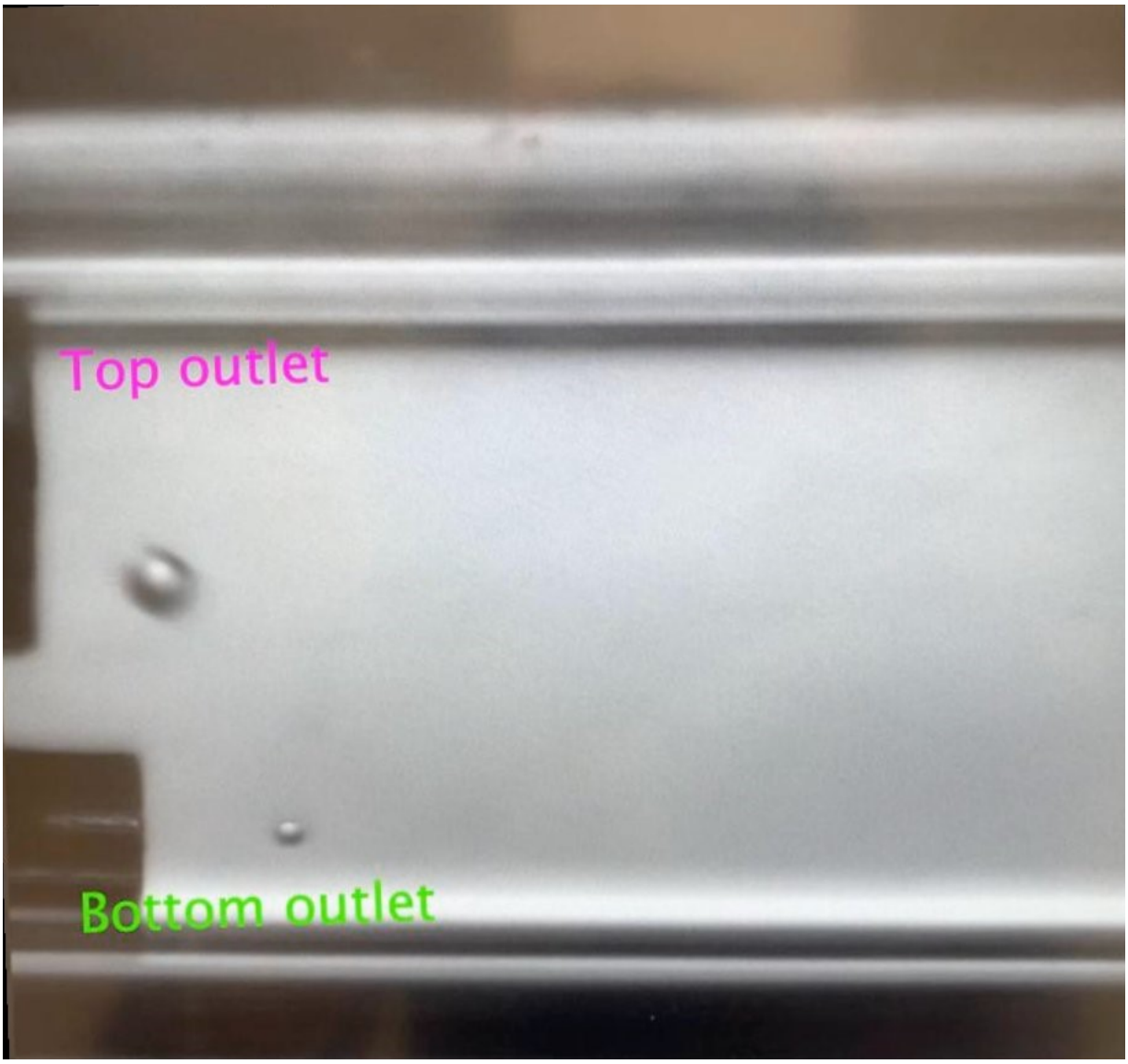

Video S1: Sorting of PS and PMMA mixture at 50 µL/min and 10 µL/min flow rates for top and bottom outlets, respectively, in a levitation media containing 0.01% of Pluronic and 75 mM Gd in PBS.

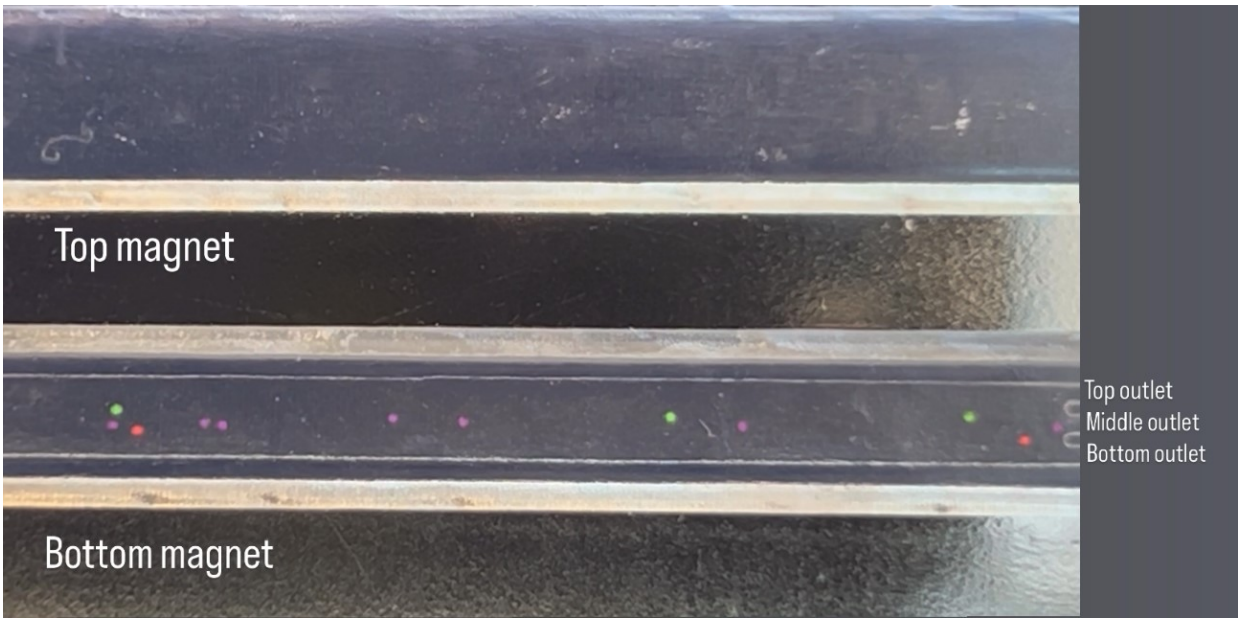

Video S2: To demonstrate the potential for isolating multiplex bead-EV complexes, we sorted three different standard density marker beads (green: 1.02, violet: 1.06, and red: 1.09 g mL^{-1}) in a 3D-printed magnetic levitation platform. The beads were levitated in a medium containing 0.01% of Pluronic and 150 mM of Gd in PBS. Flow rates for top, middle, and bottom channel were 500 µL/min, 200 µL/min, and 400 µL/min, respectively.

References

[1] Dabbagh SR, Alseed MM, Saadat M, Sitti M, Tasoglu S. Biomedical Applications of Magnetic Levitation. *Advanced NanoBiomed Research* 2022, *2* (3), 2100103.

[2] Ge S, Nemiroski A, Mirica KA, Mace CR, Hennek JW, Kumar AA, Whitesides GM, Magnetic Levitation in Chemistry, Materials Science, and Biochemistry. *Angewandte Chemie International Edition* 2020, *59* (41), 17810-17855.

[3] Ashkarran AA, Mahmoudi M, Magnetic Levitation Systems for Disease Diagnostics. *Trends in Biotechnology* 2021, *39* (3), 311-321.

[4] Yaman S, Tekin HC, Magnetic Susceptibility-Based Protein Detection Using Magnetic Levitation. *Analytical Chemistry* 2020, *92* (18), 12556-12563.

[5] Andersen MS, Howard E, Lu S, Richard M, Gregory M, Ogembo G, Mazor O, Gorelik P, Shapiro NI, Sharda AV, et al. Detection of membrane-bound and soluble antigens by magnetic levitation. *Lab Chip* 2017, *17* (20), 3462-3473.

[6] Subramaniam AB, Gonidec M, Shapiro ND, Kresse KM, Whitesides GM, Metal-Amplified Density Assays, (MADAs), including a Density-Linked Immunosorbent Assay (DeLISA). *Lab on a Chip* 2015, *15* (4), 1009-1022.

[7] Ozefe F, Arslan Yildiz A, Smartphone-assisted Hepatitis C detection assay based on magnetic levitation. *Analyst* 2020, *145* (17), 5816-5825.

[8] Durmus NG, Tekin HC, Guven S, Sridhar K, Arslan Yildiz A, Calibasi G, Ghiran I, Davis RW, Steinmetz LM, Demirci U, Magnetic levitation of single cells. *Proc Natl Acad Sci U S A* 2015, *112* (28), E3661-3668.

[9] Winkleman A, Perez-Castillejos R, Gudiksen KL, Phillips ST, Prentiss M, Whitesides GM, Density-based diamagnetic separation: devices for detecting binding events and for collecting unlabeled diamagnetic particles in paramagnetic solutions. *Analytical chemistry* 2007, *79* (17), 6542-6550.

[10] Xie J, Zhao P, Zhang C, Fu J, Turng L.-S, Current state of magnetic levitation and its applications in polymers: A review. *Sensors and Actuators B: Chemical* 2021, *333*, 129533.